Asteroid Photometric and Polarimetric Phase Effects

Karri Muinonen
University of Helsinki and Astronomical Observatory of Torino

Jukka Piironen
University of Helsinki

Yurij G. Shkuratov and Andrej Ovcharenko
Kharkov National University

Beth E. Clark
Cornell University

We review progress in the photometric and polarimetric observations of asteroids, including theoretical and experimental advances in interpreting scattering and absorption of light by asteroid surfaces. Photometric phase effects, such as the opposition effect, the overall phase function, and the so-called amplitude-phase relationship, provide insight into local physical characteristics of the surface, e.g., surface roughness and porosity, and single-particle geometrical and optical properties. Polarimetric phase effects, the negative degree of linear polarization in particular, unveil single-particle properties beyond those derivable from photometry. In order to make progress in the interpretation of the observations, it is obligatory to consider the full vector nature of light, as dictated by Maxwell's equations. We review the primary physical mechanisms for the opposition effect and the negative linear polarization. The coherent backscattering mechanism has been established to contribute to the observed opposition effects and negative linear polarizations. The traditional shadowing mechanism explanation of the opposition effect has been studied via extensive computer simulations. Laboratory photometric and polarimetric experiments with regolith-simulating samples provide an invaluable test bench for theoretical modeling. We review the progress in laboratory work, emphasizing the need for experiments with well-documented samples. We show simultaneous heuristic coherent-backscattering modeling of asteroid photometric and polarimetric phase effects for different asteroid classes. The recent findings imply enhanced future utilization of the phase effects for the benefit of asteroid science.

1. INTRODUCTION

Photometric observations for large numbers of asteroids indicate an opposition effect, a nonlinear increase of disk-integrated brightness at small solar phase angles, the angle between the Sun and the observer as seen from the asteroid (Fig. 1a). Vast sets of asteroid polarimetric observations show negative polarization, a peculiar degree of linear polarization $(I_\perp - I_\parallel)/(I_\perp + I_\parallel)$ for unpolarized incident sunlight: At small phase angles, the disk-integrated brightness component $I_\parallel$ with the electric vector parallel to the scattering plane defined by the Sun, the asteroid, and the observer predominates over the perpendicular component $I_\perp$ (Fig. 1b).

The photometric and polarimetric phase effects of asteroids have a colorful history, with important observational advances in recent years. B. Lyot discovered the negative polarization of (1) Ceres and (4) Vesta in 1934 (*Dollfus et al.,* 1989), while *Gehrels* (1956) discovered the opposition effect for the S-class asteroid (20) Massalia. In the late 1980s, *Harris et al.* (1989b) recorded narrow opposition effects for the bright E-class asteroids (44) Nysa and (64) Angelina, a discovery of paramount significance for the overall theoretical interpretation of opposition phenomena. In the 1990s, *Rosenbush et al.* (2002) made polarimetric observations of (64) Angelina, obtaining evidence for a sharp polarization feature similar to that observed for Saturn's rings by *Lyot* (1929). In our terminology, we do not distinguish between the opposition effect and "opposition spike" (narrow opposition effect) and the negative polarization surge and "polarization opposition effect" (sharp negative polarization surge).

During the past two decades, we have seen a crucial advance in theories for the physical causes of the opposition phenomena: The coherent backscattering mechanism (CBM) has been established to contribute to the photometry and polarimetry of asteroids at small solar phase angles (*Shkuratov,* 1985; *Muinonen,* 1989; *Hapke,* 1990; *Mishchenko and Dlugach,* 1993), challenging the traditional shadowing-mechanism (SM) interpretations. CBM is a multiple-scattering mechanism for scattering orders higher than the second (inclusive), whereas SM is a first-order multiple-scattering mechanism. There are several reviews on the mechanisms for the backscattering phenomena of atmosphereless

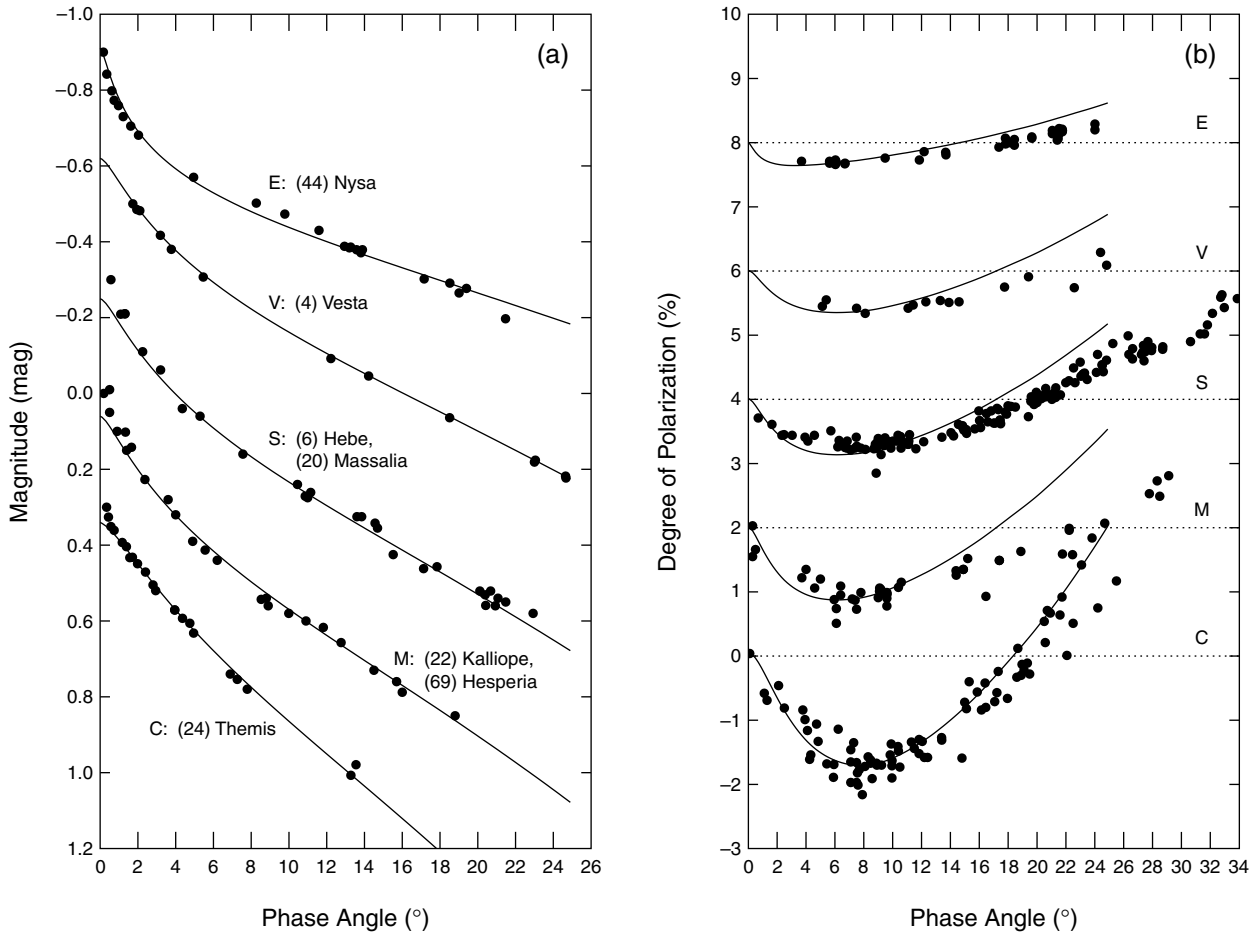

Fig. 1. **(a)** Opposition effect and **(b)** negative linear polarization observations for C-, M-, S-, V-, and E-class asteroids. For illustration, the opposition effects are presented on a relative magnitude scale, and the negative polarizations of M-, S-, V-, and E-class asteroids have been shifted upward by 2, 4, 6, and 8 vertical units respectively. The solid lines illustrate results from heuristic theoretical modeling (section 4). The polarimetric observations are from the Small Bodies Node of the Planetary Data System (http://pdssbn.astro.umd.edu/sbnhtml). The photometric observations are: (44) Nysa, *Harris et al.* (1989b); (4) Vesta, *Gehrels* (1967); (6) Hebe, *Gehrels and Taylor* (1977); (20) Massalia, *Gehrels* (1956); (22) Kalliope, *Scaltriti et al.* (1978); (69) Hesperia, *Poutanen et al.* (1985); and (24) Themis, *Harris et al.* (1989a) (see section 4 for further information on observations and theoretical modeling).

solar system bodies (e.g., *Muinonen,* 1994; *Shkuratov et al.,* 1994), and we refer the reader to these reviews for a more detailed history of, e.g., CBM and SM.

There are no exact electromagnetic solutions for light scattering by what asteroid surfaces are presumably composed of, i.e., close-packed random media of inhomogeneous particles large compared to the wavelength. The related direct problem of computing scattering characteristics for media with well-specified physical properties continues to pose a major challenge. In the inverse problem of deriving information about the physical properties of asteroid surfaces based on the observational data available, it is mandatory to make use of simplified scattering models. For example, the most popular photometric models (e.g., *Hapke,* 1986; *Lumme and Bowell,* 1981) for the inverse problem account for the single-particle albedo and phase function, the volume density (or fraction) of particles, and the roughness of the interface between the scattering medium and the free space. We note that Hapke's model has continued to be the subject of critical debate (e.g., *Mishchenko,* 1994; *Hapke,* 1996), a debate that we cannot enter into in detail. It is widely agreed that separate analyses of disk-integrated photometric or polarimetric phase effects provide two ill-posed inverse problems. However, analyzing the two datasets simultaneously may remove some of the ambiguities.

CBM for the opposition effect is described in Fig. 2a for second-order scattering. An incident electromagnetic plane wave (solid and dashed lines; wavelength λ and wavenumber $k = 2\pi/\lambda$) interacts with two scatterers A and B, which are of the order of the wavelength to hundreds of wavelengths apart, and propagates to the observer to the left. The two scattered wave components due to two opposite propagation directions between the scatterers interfere constructively in the conical directions defined by rotating the light source

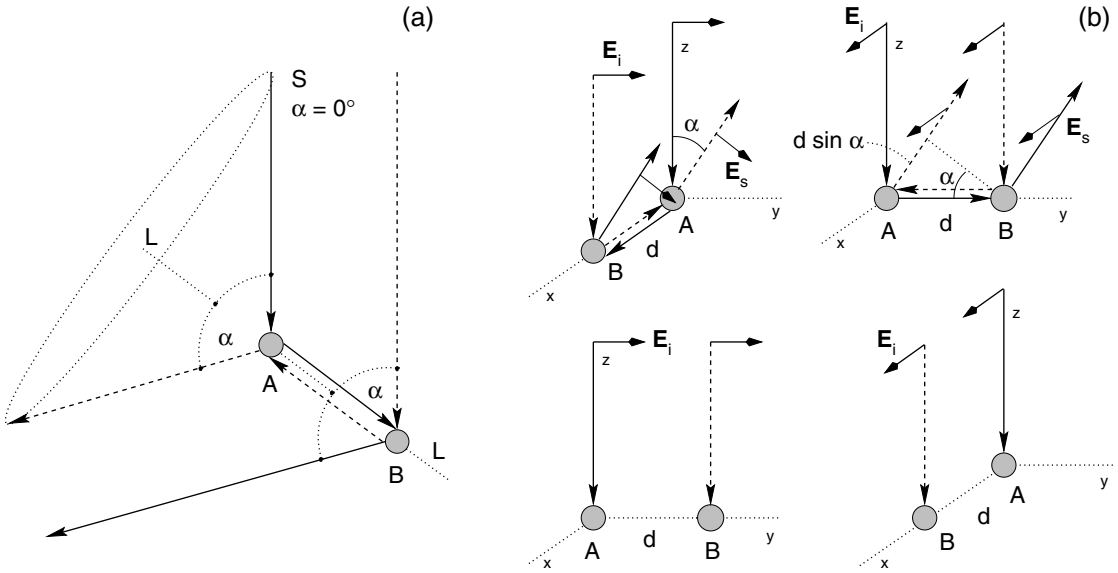

Fig. 2. **(a)** Coherent backscattering mechanism (CBM) for the opposition effect. The multiply scattering electromagnetic wave components propagating in opposite directions between the scatterers (solid and dashed lines) interfere constructively in conical directions about the axis L, always including the exact backscattering direction (phase angle $\alpha = 0°$). In other directions, the interference is arbitrary depending on the wavelength, and the distance and orientation of the first and last scattering elements. **(b)** Illustration of CBM for the negative linear polarization for unpolarized incident light. In the yz-plane in the scattering geometry leading to positive polarization, the interference depends on the phase difference kd sin α (upper right panel; k is the wave number), whereas the interference is always constructive in the geometry causing negative polarization (upper left panel). Interaction with the polarization vector parallel to the line connecting the elements is typically suppressed (two lower panels) as compared to interaction with the perpendicular polarization vector. Averaging over scatterer locations will result in an opposition effect and net negative polarization (see text).

direction S about the axis L joining the two end scatterers. We illustrate a scattering direction on the cone precisely opposite to the light source direction. Thus, the exact backward direction (phase angle $\alpha = 0°$) is on the constructive-interference cone for arbitrary locations of the two scatterers, whereas in other directions, interference varies from constructive to destructive. Three-dimensional averaging over scatterer locations results in a backscattering enhancement with decreasing angular width for increasing order of interactions, because the average distance between the end scatterers is larger for higher orders of interactions. The scattering processes can be caused by any disorder or irregularity in the medium.

CBM for the negative degree of linear polarization is explained for second-order scattering in Fig. 2b. The incident radiation is unpolarized by definition, which requires the derivation and proper averaging of the Stokes vectors corresponding to the scattered electromagnetic fields ($\mathbf{E}_s$) for two linear polarization states of an incident plane wave ($\mathbf{E}_i$). In Fig. 2b, incident polarizations parallel and perpendicular to the scattering plane (here referred to as the yz-plane) are treated in the two leftmost and two rightmost panels respectively.

Consequently, in Fig. 2b, an incident electromagnetic plane wave interacts with two scatterers A and B at a distance d from one another aligned either on the x-axis or the y-axis, while the observer is in the yz-plane. For the present geometries, the constructive interference cones of Fig. 2a reduce to the yz- and xz-planes, depending on the alignment of the scatterers. Since first-order scattering is typically positively polarized (e.g., Rayleigh scattering and Fresnel reflection), the scatterers sufficiently far away from each other ($kd = 2\pi d/\lambda \gg 1$) interact predominantly with the electric field vector perpendicular to the plane defined by the source and the scatterers (two upper panels), while interaction with the electric field vector parallel to that plane is suppressed (two lower panels). The observer in the yz-plane will detect negative polarization from the geometry in the upper left panel of Fig. 2, and positive polarization from the geometry in the upper right panel. However, the positive polarization suffers from the phase difference kd sin α, whereas the phase difference for the negative polarization is zero for all phase angles. Averaging over scatterer locations will result in negative polarization near the backward direction. Scattering orders higher than the second experience similar preferential interaction geometries, and contribute to negative polarization. As above for the opposition effect, the contributions from increasing orders of scattering manifest themselves at decreasing phase angles.

In an asteroid's surface, SM is relevant for essentially all length scales much larger than the wavelength of incident light, and is the most striking first-order multiple-scattering

effect. We can distinguish between shadowing by the rough interface between the regolith and the free space and shadowing by the internal geometric structure of the regolith. In practice, it can be difficult if not impossible to discriminate between the two shadowing contributions in disk-integrated photometric data. In both cases, SM is due to the fact that a ray of light penetrating into the scattering medium and incident on a certain particle can always emerge back along the path of incidence, whereas in other directions, the emerging ray can be blocked by other particles. The internal SM depends mainly on the volume density of the scattering medium, whereas the interfacial SM depends mainly on surface roughness (here standard deviation of the interfacial slopes). Modern modelings of the internal SM and interfacial SM are offered by, e.g., *Peltoniemi and Lumme* (1992) and *Lumme et al.* (1990) respectively.

We summarize the central questions raised by the observations of photometric and polarimetric phase dependences for asteroids as follows: (1) What are the physical mechanisms responsible for the observed phenomena? (2) What possible knowledge can be derived from the observations? (3) What observations are needed to draw conclusions about the physical mechanisms? (4) What future astronomical observations will serve to progress asteroid science? We note the fact that photometric and polarimetric observations can yield information on the physical characteristics of asteroid surfaces, but not necessarily on asteroid interiors.

The books *Asteroids* and *Asteroids II* include excellent reviews of the photometric, polarimetric, spectroscopic, mineralogical, and petrological advances through the late 1980s. *Bowell et al.* (1989) were already aware of CBM (or interference). In this chapter, we concentrate on photometric and polarimetric phase effects of asteroids. [A companion chapter (*M. Kaasalainen et al.,* 2002) focuses on the derivation of spin state, global shape, and semiempirical scattering parameters from photometric lightcurves of asteroids.] Section 2 summarizes the observational progress in groundbased photometry and polarimetry and spacecraft photometry (there is no spacecraft polarimetry on asteroids). In section 3 we review recent advances in studies of CBM and SM. Recent experimental findings are reviewed with emphasis on joint photometric and polarimetric measurements of samples relevant for asteroid research. In section 4, we present and discuss some heuristic modeling of the photometric and polarimetric phase effects. We close with future prospects in section 5.

2. OBSERVATIONAL PROGRESS

2.1. Groundbased Photometry

A vast number of asteroid photometric lightcurves valuable for phase curve studies have been published by *Harris and Young* (1989), *Harris et al.* (1989a,b), and *Wisniewski et al.* (1997). Among others, these observations are included with references in the *Asteroid Photometric Catalogue (APC)* by *Lagerkvist et al.* (2001), nearly 10,000 lightcurves are included.

The H,G magnitude system of asteroids (*Bowell et al.,* 1989) has been quite successful in general, playing a major role in asteroid science. However, it suffers from certain known drawbacks (e.g., *Lagerkvist and Magnusson,* 1990). The H,G system fails to fit the narrow opposition effects of E-class asteroids (*Harris et al.,* 1989b). Furthermore, it shows poor fits to the phase curves of certain dark asteroids: A linear fit sometimes yields smaller rms errors (e.g., *Piironen et al.,* 1994; *Shevchenko et al.,* 1996). *Verbiscer and Veverka* (1995) also analyzed the H,G magnitude system using Hapke's photometric model, and obtained photometric fits that were as good as those of the H,G system. However, we note that Hapke's photometric model has five parameters, whereas there are only two parameters in the H,G system.

Striking dependence of the photometric phase curve on the asteroid illumination and observation geometry in different apparitions was detected for certain well-observed asteroids by *Piironen et al.* (1994) and *Shevchenko et al.* (1996), yielding apparition-dependent H,G values. For (64) Angelina, such apparition dependence had already been discovered by *Poutanen* (1983). For near-Earth objects, it was observed by *Pravec et al.* (1997), and was observed for (83) Beatrix by *Krugly et al.* (1994). The phenomenon derives from variations in the physical characteristics of the surface or from global slope effects of a very irregular shape. These observations indicate that one has to be careful in analyses of photometric phase curves pertaining to different apparitions. *M. Kaasalainen et al.* (2001) suggest ways to overcome the underlying ambiguities by reducing the phase curves to so-called reference illumination and observation geometries. In addition, the empirical reduction techniques by *Muinonen et al.* (2002a) allow one to concentrate on the opposition-effect enhancement factor and angular width that can be independent of the apparition geometry.

Some of the most extensive observational campaigns of asteroids in recent years have been presented by *Mottola et al.* (1997) and *Magnusson et al.* (1996). The near-Earth asteroid (6489) Golevka (1991 JX) was observed photometrically, radiometrically, and with radar (*Mottola et al.,* 1997). Results showed that this strangely-shaped 300-m asteroid is one of the brightest ever observed (geometric albedo near 0.6). A similar campaign compiled for the near-Earth asteroid (1620) Geographos showed that this asteroid shows little variation in the physical characteristics of its surface; however, its strong lightcurve variations indicate global surface shape variations (*Magnusson et al.,* 1996). These two campaigns showed unequivocally how valuable knowledge of asteroids can be gathered via concerted efforts of several observing sites operating at complementary wavelengths.

Lagerkvist and Magnusson (1990) studied phase curves of asteroids with the help of the H,G magnitude system. Their conclusion was that the S-, C-, and M-class asteroids are well separated into different classes by their G values. Since the early 1990s, the number of asteroids for which phase curves were measured down to subdegree phase angles has increased up to about 20 and thus more than doubled, thanks to long-term observational programs by

Shevchenko et al. (1996, 1997, 2002) and *Piironen et al.* (1994). The main result from these studies is that the small-phase-angle behavior of asteroids is found to depend primarily on geometric albedo. The program by Shevchenko et al. has been devoted to observations of asteroids of various compositions at the smallest possible phase angles. As a result, detailed phase curves down to phase angles of 0.3° or less have been obtained in the V band for asteroids of P, C, G, M, S, and E classes.

Particularly interesting is the analysis of the available observational data on asteroid opposition effects by *Belskaya and Shevchenko* (2000). This survey shows unequivocally that the opposition effect differs for different asteroid taxonomic classes. This is an indication of the importance of composition in determining scattering behavior. *Belskaya and Shevchenko* (2000) found that a ratio of intensities at the phase angles of 0.3° and 5° vs. asteroid geometric albedo reveals a non-monotonic dependence of the opposition effect on albedo. The amplitude of the opposition effect decreases both for dark- and high-albedo asteroids. The largest amplitude occurs with moderate-albedo asteroids of S and M classes, which show pronounced opposition effects starting at phase angles of 5°–7°. The phase angle of 0.3° was chosen for the opposition effect estimation because, at smaller phase angles, very few observations are available. High-albedo E-class asteroids are characterized by steep and narrow opposition phenomena starting at phase angles of about 3° (*Harris et al.,* 1989b). Asteroids with similar geometric albedos show practically identical phase curves. The differences between individual phase curves for high- and moderate-albedo asteroids are on the order of the observational scatter (typically 0.02–0.03 mag).

Low-albedo asteroids show greater diversity in their phase curves. G-class asteroids tend to exhibit wide opposition effects starting at about 6°. C-class asteroids tend to show narrower and shallower effects. P- and F-class asteroids tend to show practically linear phase curves down to phase angles of about 2° (*Belskaya and Shevchenko,* 2000). Overall, results show that low-albedo asteroids with larger U-B colors tend to have stronger opposition effects.

Zappalà et al. (1990) modeled the variation in the amplitude of rotational lightcurves with solar phase angle to produce what is called the amplitude-phase relationship. They applied their model to observations of C-, M-, E-, and S-class asteroids and found that the dependence of the rotational lightcurve amplitude with solar phase is similar for C-, M-, and E-class asteroids, and is steeper for S-class asteroids. In both cases, the lightcurve amplitude increases with increasing phase angle. They found evidence that, as a first approximation, the amplitude-phase relationship was linear within 0°–30° phase angle, challenging the nonlinear dependences showing up in a similar study by *Karttunen and Bowell* (1989). Furthermore, *Karttunen and Bowell* did not report differences in the amplitude-phase relationships for S- and C-class asteroids. *Zappalà et al.* (1990) acknowledge that the discrepancies between the two studies may be due to the small observation set to which they applied their model. However, if it can be shown that the amplitude-phase relationship does map taxonomic class, then this has implications for the similarity of surface characteristics (such as porosity and roughness) within asteroid classes.

In general, extrapolation of photometric phase curves to zero phase angle (or any phase angle) depends on the assumed approximating function, and may lead to inappropriate estimates of the amplitude of the opposition effect. The very same problem is inherent in the estimation of absolute H magnitudes for near-Earth objects from large-phase-angle brightness estimates, and may thus affect the estimated numbers of such objects (see *Jedicke et al.,* 2002).

2.2. Groundbased Polarimetry

Polarimetric observations of asteroids have continued in the years following the publication of *Asteroids II*, adding significantly to the extensive campaign by *Zellner et al.* (1974), *Zellner and Gradie* (1976), and *Le Bertre and Zellner* (1980). Maximum positive polarizations have been reached for (1685) Toro by *Kiselev et al.* (1990) and for (4179) Toutatis by *Mukai et al.* (1997). The polarimetric data are collected at the Small Bodies Node of the Planetary Data System (http://pdssbn.astro.umd.edu/sbnhtml/) (*Lupishko and Vasilyev,* 1997).

Rosenbush et al. (1997) have found evidence that Io, Europa, and Ganymede — Galilean satellites of Jupiter — show negative polarization surges with sharp features at very small phase angles. They review some of the asteroid polarimetric observations, pointing out disagreements in data obtained by different research groups. *Rosenbush et al.* (2002) then provide evidence for the existence of a similar sharp feature in the negative polarization surge of (64) Angelina.

Broglia and Manara (1990, 1992, 1994) and *Broglia et al.* (1994) carried out a polarimetric study of a few large asteroids, searching for polarimetric changes with rotational phase. Such variations were found for most of the objects studied, in particular for (6) Hebe. Polarimetric observations of (6) Hebe by *Migliorini et al.* (1997) confirmed the polarization lightcurve. Because the same study found no changes in spectra at different rotational phases, it is inferred that the regolith structural variations cause the polarization light curve in this case. *Mukai et al.* (1997) found a change of polarization with rotational phase in their study of (4179) Toutatis. They concluded that this S-class asteroid exhibited substantial surface variegations.

Clark et al. (2001) provide a brief review of Earth-based observations of asteroid (433) Eros. One of the intriguing results is that although the surface of Eros exhibits globally different types of terrains, polarimetric observations in the published literature indicate no variations greater than 1 part in 40 (*Zellner and Gradie,* 1976).

Based on the polarimetric observations accumulated since late 1970s, *Lupishko and Mohamed* (1996) updated the empirical correlation rules between first the geometric albedo and the polarimetric slope at the inversion angle, and second the geometric albedo and the minimum polarization. They provided an example case where the polarimetrically determined albedo appeared to be more realistic than the

radiometrically determined one. *Cellino et al.* (1999) carried out polarimetric observations of small asteroids to obtain the polarimetric slopes and/or minimum polarizations and thus the geometric albedos that allowed them to assess the accuracy of IRAS geometric albedos for small asteroids. They saw some indications for an overestimation of these IRAS albedos.

The most considerable sets of asteroid polarimetric observations in recent years come from *Lupishko* (1999), *Lupishko and Kiselev* (1995), *Lupishko and Vasilyev* (1997), *Lupishko and Di Martino* (1998), and *Lupishko et al.* (1988, 1991, 1994, 1995, 1999), as well as *Chernova et al.* (1991, 1994). *Kiselev et al.* (1990, 1994, 1996, 1999) published polarization observations of several asteroids, including the near-Earth asteroids (1685) Toro, (1036) Ganymed, (1627) Ivar, and (2100) Ra-Shalom. In the first place, the significance of these observations lies in their quantity and rich phase angle coverage.

It is well known that the main-belt asteroid (4) Vesta shows variations of the negative-polarization degree over its surface (*Degewij et al.,* 1979; *Lupishko et al.,* 1988). New UBVRI polarimetric observations of Vesta (*Lupishko et al.,* 1999) during its rotation period confirmed the variations, showing a record high relative variation of 0.24% in the V-band degree of polarization, inversely correlated with the asteroid lightcurve. In addition, for the first time for asteroids, the observations suggested a variation of polarization-plane position angle with Vesta's rotation, maximum in the U band (8°) and minimum (2.5°) in the I band. During Vesta's rotation period, the polarization degree and position angle vary along a closed cycle, indicating a periodic change connected to Vesta's rotation. The results may be explained by the presence of orderly oriented linear features on the asteroid surface (*Lupishko et al.,* 1999), such as grooves and slopes, related to the giant 460-km crater on Vesta, recently detected by the Hubble Space Telescope (*Zellner et al.,* 1997).

The UBVRI-polarimetric observations of the Apollo asteroid (4179) Toutatis (*Lupishko et al.,* 1995) in the phase angle range of 15.8°–51.4° suggested that the Stokes parameter U (corresponding to the polarizations with the plane of vibration oriented at an angle of 45° and 135° to the scattering plane) differs from zero, when the Stokes parameter Q (corresponding to the polarizations with the plane of vibration parallel to the scattering plane and perpendicular to it) is close to zero. The corresponding values of the position angle of the polarization plane in the proper coordinate system, measured from the axis perpendicular to the scattering plane, also differs from 0° or 90° and is equal to about 45°. This would indicate an aspect of Toutatis' polarization not connected with the scattering plane. Possible causes could derive from the surface heterogeneity and complex shape. However, these observations are not confirmed by the simultaneous observations by *Mukai et al.* (1997). Furthermore, *Rosenbush et al.* (1997) emphasize that there are controversies over whether or not the Stokes U-parameter variations are real.

Kiselev et al. (1994) and *Lupishko et al.* (1995) noticed that, for S-class asteroids, the absolute value of negative polarization measured at the phase angle of 10° increases with wavelength, while the positive polarization (at 40°–90°) displays a clear decrease with wavelength. This indicates an inversion of spectral dependence of S-class asteroid polarization (*Lupishko and Kiselev,* 1995; *Lupishko and Di Martino,* 1998). In contrast, the negative polarization degree of low-albedo asteroids (1) Ceres, (704) Interamnia, and others (*Belskaya et al.,* 1987; *Lupishko et al.,* 1994) decreases with wavelength. This raises the question of whether the positive polarization degree of these asteroids increases with wavelength in a way that is the reverse of that for S-class asteroids. Measurements of polarization for Interamnia at phase angles of 10.6° (negative polarization) and 22.1° (positive, since the zero-crossing angle equals 15.7°) show that the spectral dependence of its polarization is transformed in accordance with the law described above. However, the spectral dependence of positive polarization of C-asteroids (2100) Ra-Shalom at the phase angle of 60° (*Kiselev et al.,* 1999) and (1580) Betulia at 39° (*Tedesco et al.,* 1978) reveals a small reduction of polarization with increasing wavelength.

2.3. Spacecraft Photometry

Since the time of *Asteroids II*, disk-resolved observations by two spacecraft, *Galileo* and *NEAR Shoemaker*, have dramatically increased our understanding of asteroid spectrophotometric properties. The *Galileo* spacecraft flew by asteroids (951) Gaspra and (243) Ida in the early 1990s, obtaining images and spectroscopy. *Helfenstein et al.* (1994, 1996) have performed extensive analyses of these observations based on Hapke's photometric model. Generalized, these analyses provide a detailed examination of the photometric behavior of S-class asteroids. In addition, the Helfenstein et al. work on Gaspra and Ida provided the first quantitative analyses of the distribution and magnitude of asteroid surface color variations at broad-band wavelengths in the visible. These analyses showed that asteroid surface color variations occur on small and large spatial scales, and can be linked with surface processes, such as cratering.

The first of the *NEAR Shoemaker* mission targets, C-class asteroid (253) Mathilde, has been photometrically analyzed by *Clark et al.* (1999). Looking at photometric properties at a broadband wavelength of 0.7 μm, Clark et al. showed that Mathilde is remarkably uniform in albedo and other photometric properties on spatial scales of 1 km or more. The main *NEAR Shoemaker* mission target, S asteroid (433) Eros, has also been analyzed in terms of its photometric and spectrophotometric properties across a wide wavelength range of 0.55–2.4 μm, and a wide phase angle range of 1.2° to 111° (*Clark et al.,* 2002; *Domingue et al.,* 2002; *Veverka et al.,* 1999, 2000).

While most spacecraft studies of asteroid photometric properties have used broadband visible wavelengths, one study in particular has examined narrow-band multiwave-

length observations of (433) Eros. Such a multiwavelength approach is useful in isolating model parameter effects because some purely geometric scattering model parameters should not be wavelength-dependent. Specifically, near-infrared spectrometer observations (0.8–2.4 μm) of Eros have been compared with the Hapke photometric model at phase angles ranging from 1.2° to 111.0° and at spatial resolutions of 1.25–5.5 km/spectrum (*Clark et al.,* 2002). A 15% increase in the 1-μm band depth was observed at high phase angles. In contrast, only a 5% increase in continuum slope from 1.5 to 2.4 μm and essentially no difference in the 2-μm band depth were observed at higher phase angles. These contrasting phase effects imply that phase-dependent differences must be accounted for in the computation of parametric measurements of 1- and 2-μm band areas. Whole-disk phase curves derived from the models indicate that Eros exhibits phase reddening of 8–12% across the phase angle range of 0°–100° (Fig. 3). Phase reddening is most severe for wavelengths inside the 1.0- and 2.0-μm silicate absorption features. These results agree in both sense and magnitude with the laboratory study of silicate materials performed by *Gradie et al.* (1980). It is interesting that the phase reddening effects are not accompanied by variations in the single-particle phase functions, implying that single-scattering albedo, and hence multiple scattering, are more important controls of phase reddening than is the single particle phase function.

In the *Clark et al.* (2002) study, two of five Hapke model parameters exhibited a notable wavelength dependence: (1) The single-scattering albedo mimics the spectrum of Eros, and (2) there is a decrease in angular width of the opposition surge with increasing wavelength from 0.8 to 1.6 μm. Such opposition surge behavior is not adequately modeled with the shadow-hiding Hapke model, consistent with coherent backscattering phenomena near zero phase.

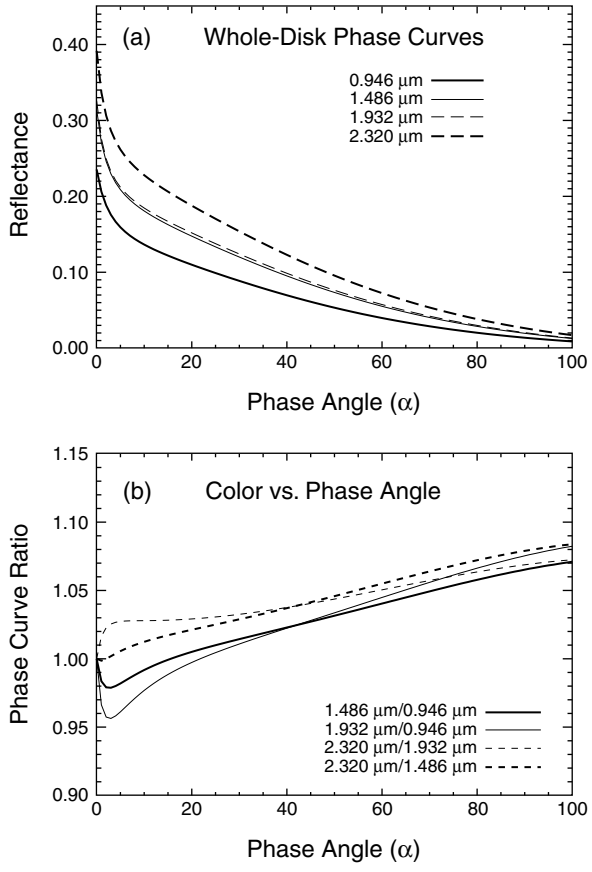

Fig. 3. Disk-integrated multiwavelength opposition effects of asteroid Eros as derived from the disk-resolved observations of *NEAR Shoemaker*.

3. THEORETICAL AND EXPERIMENTAL ADVANCES

Theoretical advances in asteroid photometry and polarimetry concern the fundamental physical understanding of the opposition effect and negative polarization. These advances have been supported by numerous laboratory measurements.

3.1. Coherent Backscattering Mechanism

Based on both theoretical and experimental findings, *Shkuratov* (1985) suggested that the coherent backscattering mechanism is relevant for the opposition effect and negative polarization of atmosphereless solar system bodies. *Muinonen* (1989, 1990) solved the electromagnetic scattering problem of two interacting dipole particles analytically and showed that the coherent backscattering opposition effect is accompanied by negative polarization. He offered a physical explanation independent of the work by *Shkuratov* (1985). Using rigorous T-matrix computations, *Mishchenko* (1996b) showed unequivocally that CBM played a role in light scattering by two interacting spherical particles (cf. *Muinonen,* 1989). *Lumme et al.* (1997) saw tentative clues of CBM in their application of the discrete-dipole approximation to scattering by dense clusters of spherical particles.

Furthermore, *Muinonen et al.* (1991) showed unequivocally that the opposition effect and negative polarization follow naturally when the electromagnetic scattering problem of a dipole particle above a plane-parallel interface of solid optically isotropic and homogeneous medium is treated exactly. Based on the resulting shallow and narrow negative polarizations, they suggested that interactions among the small-scale inhomogeneities are more important than those between small-scale inhomogeneities and surface elements. It is interesting that the morphology of the observed asteroid opposition effects and negative polarizations is already apparent in their example computations. *Muinonen and Lumme* (1991) (see also *Shkuratov,* 1989; *Videen,* 2002) showed that second-order external Fresnel reflection from two spherical particles is large compared to the wavelength revealed signatures of the opposition effect and negative polarization. However, the intensity component due to ex-

ternal Fresnel reflections is only a fraction of the total intensity scattered by an asteroid's surface.

Shkuratov and his colleagues continued their theoretical investigations of the opposition effect and negative polarization (e.g., *Shkuratov,* 1991; *Zubko et al.,* 2002). In addition, computer modeling of ray tracing in particulate media, including simulations in the opposition phenomena context, began (e.g., *Zubko et al.,* 2002; *Shkuratov et al.,* 2002). *Hapke* (1990, 1993) continued theoretical work on scattering of light, with CBM receiving particular attention. *Kolokolova et al.* (1993) provided statistical evidence that CBM was the primary contributor to the negative polarization for media of subwavelength-sized scatterers.

Mishchenko and Dlugach (1993) and *Mishchenko* (1996a) concentrated on modeling CBM for discrete random media of scatterers including polarization effects. The former study offered advanced CBM modeling for the opposition effect of E-class asteroids (see also *Shkuratov and Muinonen,* 1992), while the latter study described extensive computations of various multiple scattering parameters at the exact backscattering direction using the reciprocity principle of electromagnetic scattering. *Mishchenko et al.* (2000) made use of the analytical theories by *Ozrin* (1992) and *Amic et al.* (1997) to compute coherent backscattering by conservative media of Rayleigh scatterers. They were able to offer reference results, that is, accurate predictions for the values of the amplitude and width of the opposition effect and the shape and depth of the negative polarization surge.

Tishkovets (2002) and *Tishkovets et al.* (2002) studied CBM for layer-type and semi-infinite discrete random media of absorbing scatterers including multiple scattering up to the second order. They theorized that the considerable width of the negative polarization surge as compared to the photometric surge is due to the longitudinal component of the electromagnetic near-fields in the discrete scattering medium.

Very recently, *Muinonen* (2002; see also *Muinonen et al.,* 2002b) put forward a computational algorithm for coherent backscattering by absorbing and scattering media. The algorithm mimics radiative transfer but, for each multiple scattering event, it additionally computes the coherent backscattering contribution. The algorithm is currently under further development, and the first results are in accordance with the findings by *Muinonen et al.* (1991), extending and not disagreeing with the reference results by *Mishchenko et al.* (2000).

3.2. Shadowing Mechanism

In their ray-tracing simulations for close-packed random media of spherical particles, *Peltoniemi and Lumme* (1992) noted that the radiative transfer models by *Hapke* (1986) and *Lumme and Bowell* (1981) can be severely in error for close-packed random media of spherical particles. In particular, the error can be considerable, even a factor of several, for grazing emergence of rays.

Stankevich et al. (1999) carried out computer simulations of shadowing for semi-infinite plane-parallel media of close-packed spherical particles. They emphasized that it is nontrivial to generate semi-infinite close-packed media of constant volume density. *Muinonen et al.* (2001) studied SM for clusters of opaque spherical particles. By increasing the number of constituent particles, they revealed the gradual increase of the opposition effect due to shadowing, thus providing supporting theoretical evidence for an SM opposition effect. However, for realistic particle volume fractions, the angular widths of the opposition effects were typically larger than those observed for asteroids.

In his Ph.D. dissertation, *Peltoniemi* (1993a) completed an extensive geometric optics study of scattering of light by planetary regoliths. *Peltoniemi* (1993b) and *Stankevich et al.* (2002) offered three-dimensional Gaussian modeling for the planetary regolith geometry. For such random media, Stankevich et al. studied shadowing in orders higher than the first, concluding that those shadowing contributions are negligible as compared to the first-order one [in agreement with *Esposito* (1979)].

Shepard and Campbell (1998) utilized a fractal surface model in the simulation of light scattering from rough surfaces. They compared their model to Hapke's and discussed the meaning of roughness in problems concerning scattering of light. *Hillier* (1997) put forward a double-layer radiative transfer model to explain the opposition effect using only SM. He concluded that it may not be necessary after all to invoke CBM to explain the observations. The possibility of an additional enhancement of SM was considered by *Shkuratov and Helfenstein* (2001). They hypothesized that a fractallike, hierarchical structure of asteroid surfaces could enhance the SM contribution to the opposition effect.

3.3. New Laboratory Results

Photometric studies by *Oetking* (1966) continue to deserve attention due to the completeness of the choice of samples and intriguing variety of results. The results of this study have been very useful in planning new laboratory experiments of light scattering.

Extensive laboratory photometric and polarimetric studies were carried out by *Shkuratov et al.* (1992) and *Shkuratov and Opanasenko* (1992) at the phase-angle range of 2°–50°. They showed, in particular, that the depth and the inversion angle of negative polarization depend strongly on the microscopic optical inhomogeneity of the surfaces, e.g., a mixture of smoked MgO and soot gives a minimum polarization down to –3.5% and an inversion angle reaching up to 35° (*Shkuratov,* 1987).

Laboratory measurements have been rare at phase angles <1°. Recently, simultaneous polarimetric and photometric measurements were carried out at phase angles covering 0.2°–4° for unpolarized incident light (*Shkuratov et al.,* 1999, 2002; *Ovcharenko and Shkuratov,* 2000). The instrument was calibrated with a comparable photometer at the Jet Propulsion Laboratory (*Nelson et al.,* 1999). Samples with controlled structural characteristics and albedos were studied. Several important results for testing theoretical

models were obtained in the laboratory studies by *Shkuratov et al.* (2002).

First, the volume density of the scattering medium can dramatically influence the negative polarization. Figure 4 shows data for coatings of smoked MgO before and after compressing. Due to compression, the angle of minimum polarization shifts from the small phase angle of 1° up to the phase angle range of 5°–10°, changing the negative surge from asymmetric to regular and symmetric. The width of the opposition effect increases along with the compression.

Second, a strong particle-size dependence of the negative polarization for powdered dielectric surfaces was found for particle-size separates of Al_2O_3 studied by *Nelson et al.* (2000). Data for the separates of 0.1, 0.5, 1.0, 3.2, and 12.1 μm are shown in Fig. 4. These separates have almost the same high albedo. For grain sizes larger than 1 μm, the depth of the negative polarization does not exceed 0.25%. The smallest fractions of 0.1 and 0.5 μm reveal similar dependences with the minimum near 1.6° and amplitude of 0.8%. The polarization of the 1.0 μm fraction is located between the fine and coarse powdered samples. Figure 4 demonstrates the systematic evolution of polarimetric phase

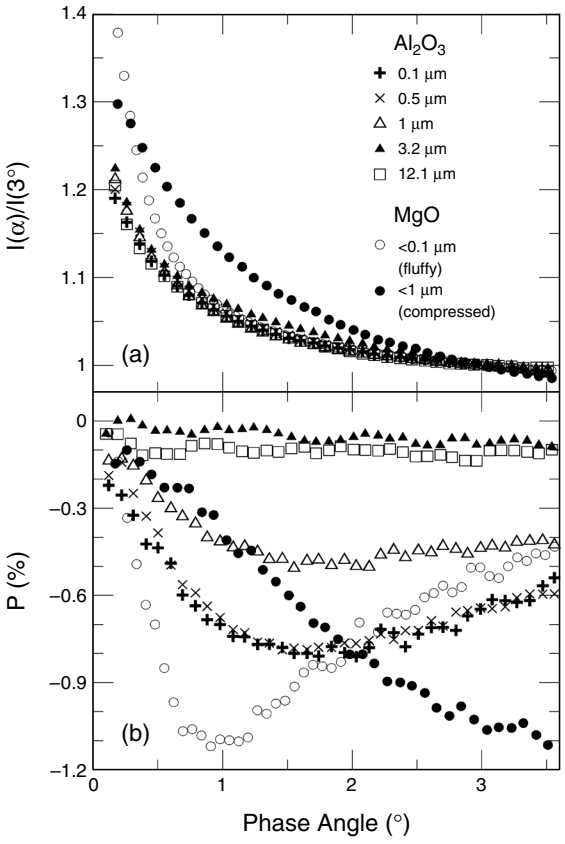

Fig. 4. Phase functions of brightness and polarization degree for plane-parallel coatings of smoked MgO before and after compression, as well as for particle-size separates of Al_2O_3 powder (*Shkuratov et al.,* 2002), in the nadir-imaging geometry.

dependences along with particle size. As for the photometric data, the phase functions of the samples of 0.1, 0.5, 1.0, and 12.1 μm are fairly inert to the particle size. The measurements of Al_2O_3 particle-size separates thus provide an example where the negative polarization is a more sensitive particle-size discriminator than the opposition effect. Third, *Ovcharenko and Shkuratov* (2000) found a MgO-like surge of negative polarization for soot.

Hapke et al. (1993, 1998) put forward a hypothesis that experimental measurements for the phase dependences of the so-called linear and circular polarization ratios could discriminate between CBM and SM contributions to the opposition effect of the Moon. In the former work, they concluded that CBM was the primary cause of the opposition effects of atmosphereless solar system bodies, but in the latter, they found evidence for SM contributions. Further theoretical and experimental studies are needed to assess these interesting analyses. *Nelson et al.* (1999, 2000) published small-phase-angle measurements of Al_2O_3 powders. They confirmed a dependence of opposition effect on the size of particles. The maximum opposition effect was seen when the particle sizes were a few times the wavelength. *Shepard and Arvidson* (1999) studied basalt samples and suggested that the opposition surge and negative polarization found in pulverized samples is caused by CBM. Also relevant for asteroid studies, the AMIE microcamera [J-L. Josset, PI; cf. *Muinonen et al.* (2002c)] onboard the ESA SMART-1 mission to the Moon (launch in February 1, 2003) should soon contribute to our general understanding of the opposition effect.

Capaccioni et al. (1990) published numerous laboratory phase curves of terrestrial rocks and meteorites. The laboratory phase curves at moderately large phase angles are qualitatively comparable to the observed phase curves of asteroids. *Piironen et al.* (1998) measured single-particle albedos of meteorites (for particle sizes from a few tens of micrometers upwards) using the device described in *Sasse et al.* (1996). Their results indicated fairly high single-particle albedos that did not show a strong dependence on particle size. *Kamei and Nakamura* (2002) have carried out extensive photometric measurements of various meteorites and other powdered materials. Their estimates of the single-particle albedos were in agreement with those measured by *Piironen et al.* (1998).

McGuire and Hapke (1995) studied scattering of light by large particles in the laboratory. They concluded that large particles are mostly backward scattering (excluding forward diffraction), which is a logical result because their analog particle sizes were on the order of 1 cm. Recently, *Volten et al.* (2001) carried out extensive scattering matrix measurements for mineral aerosol particles, for example, and were able to obtain similar scattering matrices from ray-optics simulations with Gaussian random particles, i.e., stochastically shaped particles described by the lognormal distribution with given mean (radius), standard deviation, and correlation function (e.g., *Muinonen,* 2000). The measurements were then studied further by *Nousiainen et al.* (2002),

who were able to improve the ray-optics analyses by *Volten et al.* (2001) and interpret the measurements using a modified ray-optics approximation, where the Gaussian particles are assumed to consist of an optically isotropic and homogeneous medium with both specular and Lambertian surface elements (in addition, Lambertian internal interfaces were assumed). Long-term experimental work on scattering by snow (*Piironen et al.,* 2000) has now been extended by *S. Kaasalainen et al.* (2002) to experimental laboratory work on backscattering characteristics of various regolith-type samples.

4. DISCUSSION

We now return to asteroid photometric and polarimetric observations and theoretical modeling in Fig. 1. As for the photometric observations in Fig. 1a, there are several important details. The observations of (44) Nysa are referred to as the mean light level of the lightcurve, including a correction of 0.0007 mag/° subtracted from the observations for phase angles before the opposition and added to the observations after the opposition [*Harris et al.* (1989b); correction attributed to changing illumination and observation geometry]. The observations of (4) Vesta are referred to as the mean light level (*Gehrels,* 1967), and so are the observations of (20) Massalia (*Gehrels,* 1956) and (24) Themis [*Harris et al.* (1989a), using Fourier analysis]. The observations of (6) Hebe are referred to as the maximum light level (*Gehrels and Taylor,* 1977), and combined from several apparitions using shifts based on an optimum fit using the H,G magnitude system (*Bowell et al.,* 1989); naturally, the shifts should be recomputed here, but for the current purpose of illustration, the H,G shifted dataset will suffice [it overlaps nicely with the data for (20) Massalia]. The observations of (22) Kalliope represent the maximum light level (*Scaltriti et al.,* 1978), as well as the observations of (69) Hesperia (*Poutanen et al.,* 1985). Additionally, the phase curve pairs for S-class asteroids and M-class asteroids have been combined graphically by introducing essentially arbitrary shifts along the magnitude axis. This simple combination technique is appropriate for the simplified theoretical modeling that follows.

The observed photometric and polarimetric phase effects in Fig. 1 provide an immediate constraint on the possible physical mechanisms involved: Laws of physics dictate that the first derivatives at the zero phase angle must vanish. The observations indicate that this vanishing must take place at very small phase angles not covered by the data. To produce such sharp features, the underlying physical mechanism must extend over a large number of wavelengths of incident light. Both SM and CBM are then eligible to explain the photometric observations at small phase angles (Fig. 1a), but SM suffers from the drawback of not being proven to cause negative polarization (Fig. 1b). Furthermore, SM would seem to require unrealistically small particle volume densities to produce sufficiently narrow opposition effects (*Muinonen et al.,* 2001). We thus note that, on one hand, there is so far no theoretical, observational, or experimental evidence against CBM as the mechanism for the opposition effect and negative polarization surge, whereas on the other hand, there is no compelling evidence for SM providing negative polarization.

Figure 1 shows heuristic, perhaps provocative modeling of the opposition effect and negative polarization of C-, M-, S-, V-, and E-class asteroids using Monte Carlo computations for coherent backscattering (*Muinonen,* 2002; *Muinonen et al.,* 2002b). The numerical technique relies on the reciprocity principle for electromagnetic scattering, allowing a renormalization of the coherent backscattering contributions at each multiple-scattering event. The technique is currently available for finite/semi-infinite plane-parallel media and spherical media of scatterers, as well as for semi-infinite plane-parallel media embedded in a semi-infinite optically isotropic and homogeneous host medium. At the present, numerical studies have begun, and further refinements and applications are expected in the future.

Coherent backscattering is here computed for a plane wave (wavelength $\lambda = 2\pi/10$ μm) normally incident on a semi-infinite medium of discrete Rayleigh scatterers with single-scattering albedos of 0.9 and medium mean-free-path length of $\ell = 1, 2, 3, \ldots, 50$ μm. For Rayleigh scatterers, the single-scattering albedo chosen roughly results in a maximum opposition effect amplitude as well as a maximum depth of the negative polarization surge. Each computation used 5×10^4 rays.

In Fig. 1, an ad hoc exponential weighting scheme of $\exp(-\ell/L)$ has been applied to the numerical results in all cases with L = 1.0, 2.0, 2.0, 2.0, and 6.0 μm for the C-, M-, S-, V-, and E-class curves respectively. The weighting scheme derives from the idea that, rather than modeling the random scattering medium using a single mean free path only, we allow a distribution of mean free paths and thus physical characteristics on asteroid surfaces. Additionally, the CBM computations have been multiplied by a linear function $1 - K\alpha$ (e.g., mimicking SM), where K = 0.021/°, 0.017/°, 0.015/°, 0.013/°, and 0.009/° for C-, M-, S-, V-, and E-class curves respectively. Finally, because of the excess depth of the negative polarization surges computed (see below), for comparison with the polarimetric observations, they have been divided by the scaling "fudge factors" of 1.5, 2.3, 3.0, 4.0, and 7.2 in a fashion similar to the comparison of computations and experimental data in *Mishchenko et al.* (2000).

We point out that, as evident in Fig. 1, we cannot obtain excellent fits for both the photometric and polarimetric phase effects: There are problems in simultaneously producing the amplitude of the opposition effect and the width of the negative polarization surge. We have chosen to treat the photometric and polarimetric observations in a fair way by showing equally good or poor fits for both sets of observations. Based on the present computations, we note that the asymmetric polarization surge implied for E-class asteroids is in overall agreement with the observations by *Rosenbush et al.* (2002) and that the best fits are obtained for C-class

asteroids (with the smallest polarization scaling factor). The most severe fitting problems are encountered in the photometry and polarimetry of S- and M-class asteroids.

We note that multiple Rayleigh scattering results in negative polarization surges that are too deep and too narrow to fully explain the current observations. We can predict that better agreement with both photometric and polarimetric data can be obtained by incorporating multipole scatterers of degrees higher than the second (Rayleigh scatterers are pure electric dipole scatterers). Such multipole scatterers provide more forward-scattering and less positively polarizing scattering phase matrices, in agreement with what is needed to improve the present modeling. Such phase matrices can exhibit both negative and positive polarization, and their interplay with CBM and the observed negative polarization surges are topics of future research.

Furthermore, there are two primary physical mechanisms that could extend the negative polarization surge toward larger phase angles without affecting the opposition effect significantly at smaller phase angles: (1) diffraction connected to SM and affecting the CBM contributions from well inside a densely packed discrete medium, (2) divergence connected to CBM contributions from inhomogeneities inside otherwise optically isotropic and homogeneous particles of the scattering medium. The second mechanism has already been seen to widen the negative polarization surges (*Muinonen,* 2002).

It is probable that SM is contributing in a moderately nonlinear way to the photometric phase effect, thus improving the agreement between the observations and theoretical computations. The polarimetric scaling factors offer at least a clue that SM cannot be solely responsible for the poorness of the current fits: Shadowing contributions should be smaller for brighter asteroids, whereas the scaling factors are larger for brighter asteroids. One more caveat is still due. We have made use of a single value for the single-scattering albedo, whereas albedo obviously varies among the asteroid classes presently studied. In effect, the scaling factors probably reflect the current use of a fixed single-scattering albedo. Consistent with earlier analyses, the linear photometric slopes (parameter K above) become steeper with darker asteroids whose photometric phase effects, in agreement with decreased multiple scattering, are more strongly affected by internal and interfacial SM.

5. FUTURE PROSPECTS

5.1. Theory and Experiments

The coherent backscattering and shadowing mechanisms appear to be primarily responsible for the observed phase effects (question 1 in section 1). Based on the present discussions, we can indicate a direction for further theoretical studies of the coherent backscattering mechanism: For scattering models to be used in inverse light-scattering problems of asteroids, the coherent backscattering contributions could be computed with the help of electromagnetic field expansions in terms of vector spherical harmonics. Such field expansions yield scattering phase matrices that account for general multipole radiation. How such expansions are related to the physical properties of the scattering media is a fundamental problem of physics that is ripe for development.

We predict that further theoretical and computational progress in light scattering by natural particles will allow a construction of extensive electronic databases of scattering models. Such models can be rapidly applied in the interpretation of asteroid observations, mimicking the readiness of analytical theoretical models such as the Lumme-Bowell and Hapke models, for example. In addition, theoretical models can, in part, be applied in the interpretation of radar, X-ray, and spectroscopic observations of asteroids. During the next decade, we envisage an update to the current H,G magnitude system of asteroids. This update will involve new parameters, new definitions, and our new understanding of the physics involved.

The discussions in section 4 give hints about the possible knowledge (question 2 in section 1) that can be derived from the photometric and polarimetric observations of asteroids. Indeed, it can be promising that the simple modeling was not fully successful: All the observational data together appear to put constraints on the physical characteristics of the single scatterers themselves and the media composed of them.

In laboratory experiments, the physical properties of materials relevant for asteroid studies, such as meteorites, need to be quantitatively measured. Such characterization should include both geometrical and optical properties of the particle surfaces as well as their interiors. In particular, the source of absorption in such materials needs to be assessed. Is the absorption of light due to the optically homogeneous and isotropic host matter, or due to the disorder embedded in it? What are the typical distributions of complex refractive indices? From mineralogical and spectroscopic studies (see *Gaffey et al.,* 2002), we know that these questions are complex and highly wavelength-dependent. It is a challenge for future studies to explain the curious color effects at small phase angles in Fig. 3.

It is probable that wavelength-sized void scatterers are inherent in media of close-packed particles with complicated internal structures. It is intriguing that such void scatterers have single-scattering albedos equal to unity, being potential contributors to coherent backscattering mechanism and the overall brightness in dark media consisting of small particles (e.g., soot).

Additional experiments are needed for coherent backscattering and shadowing by meteorite and other naturally occurring materials. Near-future ICAPS light-scattering experiments in microgravity on board the International Space Station can offer valuable insight (*Blum et al.,* 1999). Where does the main contribution of coherent backscattering come from: from the internal or surface structures of single particles that are large compared to the wavelength, or from interactions between small wavelength-scale particles? Is there a way to distinguish between these two contributions?

How much does diffraction affect the shadowing mechanism? Such experiments will profit from simultaneous theoretical computations.

5.2. Observations

While the recent past has been eye-opening in terms of theoretical advances, we envisage future focus on the observations and the inverse problems they provide. The inverse problems benefit from sophisticated scattering models that should be available soon. Empirical analyses of photometric and polarimetric phase effects could result in viable means for physical classification of asteroids.

For revising the magnitude system for asteroids (question 4 in section 1), it would be important to obtain photometric observations for near-Earth asteroids of various classes in several wavelength bands at wide phase angle ranges, spanning from very large to very small phase angles. The photometric observations could be accompanied by polarimetric observations in order to develop a suitable polarimetric system for asteroids, and contribute to our understanding of the physical mechanisms involved (question 1 in section 1). It is, however, important to realize that developing the magnitude system requires particular caution. As near-Earth asteroids are small, their surface characteristics can differ from those of the generally larger main-belt asteroids, e.g., with small particles missing entirely, giving rise to substantially differing phase curves even for asteroids belonging to the same taxonomic classes.

In the near future, asteroid astrometry and photometry will become intertwingled by, for example, asteroid photocenters differing from asteroid barycenters, and the solar electromagnetic radiation pressure and Yarkovsky thermal emission forces acting on the asteroids (see *Bowell et al.,* 2002). Thus, a full utilization of highly accurate astrometric observations, for example, those planned for the ESA cornerstone mission GAIA (launch around 2011), will benefit from enhanced photometric observation campaigns of large numbers of asteroids (and vice versa).

To move forward with theoretical modeling, we recommend small-phase-angle polarimetric and photometric observations of dark asteroids (question 3 in section 1). Are there indications of sharp but suppressed parts of the opposition effect? Do we see a saturation or even a decrease of the amplitude of negative polarization? Are there sharp features at small phase angles in the polarimetry of S- or M-class asteroids? Narrow-band multiwavelength polarimetric observations would help interpret the color effects in Fig. 3.

As for bright asteroids, we recommend continued polarimetric observations of Angelina and Nysa in order to decisively determine their polarization characteristics. Are there apparition dependences in the negative polarization characteristics? Whether the Stokes parameter U is typically nonzero at the zero-crossing angle of polarization requires further observational work. Reaching an observational consensus on issues like this is crucial for the overall credibility of modern asteroid polarimetry. In essence, we call for a calibration campaign of asteroid polarimetry.

A major breakthrough is still pending in the observationally challenging circular polarimetry of asteroids. It could yield valuable information about an asteroid's spin state, shape, and microscopic physical properties beyond photometry and linear polarimetry.

Acknowledgments. We are grateful to D. Domingue and I. Belskaya for extensive constructive reviews of an early version of the chapter, and A. Cellino for his guidance with the chapter contents. A. Harris (JPL) offered valuable help with the photometric observations, while V. Rosenbush, D. Lupishko, and N. Kiselev helped us review the state of the art in polarimetric observations. We appreciate theoretical remarks by K. Lumme and J. Peltoniemi, experimental comments by A. Nakamura, and observational contributions by V. Shevchenko. G. Videen offered much-respected cricitism on the figures explaining CBM. Additional comments were offered by M. Kaasalainen, T. Nousiainen, and S. Kaasalainen. K.M. is grateful to the Astronomical Observatory of Torino for hospitality during his sabbatical stay and for the Academy of Finland for financial support. This research is supported in part by INTAS Grant No. 2000-0792.

REFERENCES

Amic E., Luck J. M., and Nieuwenhuizen Th. M. (1997) Multiple Rayleigh scattering of electromagnetic waves. *J. Phys. I, 7,* 445–483.

Belskaya I. N. and Shevchenko V. G. (2000) Opposition effect of asteroids. *Icarus, 147,* 94–105.

Belskaya I. N., Lupishko D. F., and Shakhovskoj N. M. (1987) Negative-polarization spectra for five asteroids. *Sov. Astron. Lett., 13,* 219–220.

Blum J., Cabane M., Henning T., Holländer W., Levasseur-Regourd A.-C., Lumme K., Marijnissen J., Muinonen K., Poppe T., Prodi F., Wagner P., and Worms J.-C. (1999) Research with small particles onboard the ISS. In *2nd European Symposium on Utilisation of the International Space Station* (A. Wilson, ed.), pp. 285–289. ESA SP-433.

Bowell E., Hapke B., Dominque D., Lumme K., Peltoniemi J. I., and Harris A. W. (1989) Application of photometric models to asteroids. In *Asteroids II* (R. P. Binzel et al., eds.), pp. 524–556. Univ. of Arizona, Tucson.

Bowell E., Virtanen J., Muinonen K., and Boattini A. (2002) Asteroid orbit computation. In *Asteroids III* (W. F. Bottke Jr. et al., eds.), this volume. Univ. of Arizona, Tucson.

Broglia P. and Manara A. (1990) A search for rotational variations in the optical polarization of 3 Juno and 7 Iris. *Astron. Astrophys., 237,* 256–258.

Broglia P. and Manara A. (1992) A study of the polarimetric lightcurve of the asteroid 16 Psyche. *Astron. Astrophys., 257,* 770–772.

Broglia P. and Manara A. (1994) Polarimetric observations of 51 Nemausa during its 1991 apparition. *Astron. Astrophys., 281,* 576–578.

Broglia P., and Manara A., and Farinella P. (1994) Polarimetric observations of (6) Hebe. *Icarus, 109,* 204–209.

Capaccioni F., Cerroni P., Barucci M. A., and Fulchignoni M. (1990) Phase curves of meteorites and terrestrial rocks: Labo-

ratory measurements and application to asteroids. *Icarus, 83,* 325–348.

Cellino A., Gil Hutton R., Tedesco E. F., Di Martino M., and Brunini A. (1999) Polarimetric observations of small asteroids: Preliminary results. *Icarus, 138,* 129–140.

Chernova G. P., Lupishko D. F., Shevchenko V. G., Kiselev N. N., and Saljes R. (1991) Photometry and polarimetry of asteroid 47 Aglaja. *Kin. Phys. Neb. Tel., 7,* 20–26 (in Russian).

Chernova G. P., Lupishko D. F., and Shevchenko V. G. (1994) Photometry and polarimetry of asteroid 24 Themis. *Kin. Phys. Neb. Tel., 10,* 45–49.

Clark B. E., Veverka J., Helfenstein P., Thomas P. C., Bell J. F. III, Harch A., Robinson M. S., Murchie S. L., McFadden L. A., and Chapman C. R. (1999) NEAR photometry of asteroid 253 Mathilde. *Icarus, 140,* 53–65.

Clark B. E., Lucey P., Helfenstein P., Bell J. F. III, Peterson C., Veverka J., McConnochie T., Robinson M., Bussey B., Murchie S., Izenberg N., and Chapman C. (2001) Space weathering on Eros: Constraints from albedo and spectral measurements of Psyche crater. *Meteoritics & Planet. Sci., 36,* 1617–1638.

Clark B. E., Helfenstein P., Bell J. F. III, Peterson C., Veverka J., Izenberg N. I., Domingue D., Wellnitz D., and McFadden L. (2002) NEAR infrared spectrometer photometry of asteroid 433 Eros. *Icarus, 155,* 189–204.

Degewij J., Tedesco E. F., and Zellner B. (1979) Albedo and color contrasts on asteroid surfaces. *Icarus, 40,* 364–374.

Dollfus A., Wolff M., Geake J. E., Lupishko D. F., and Dougherty L. M. (1989) Photopolarimetry of asteroids. In *Asteroids II* (R. P. Binzel et al., eds.), pp. 594–616. Univ. of Arizona, Tucson.

Domingue D. L., Robinson M., Carcich B., Joseph J., Thomas P., and Clark B. E. (2002) Disk-integrated photometry of 433 Eros. *Icarus, 155,* 205–219.

Esposito L. W. (1979) Extensions to the classical calculation of the effect of mutual shadowing in diffuse reflection. *Icarus, 39,* 69–80.

Gaffey M. J., Cloutis E. A., Kelley M. S., and Reed K. L. (2002) Mineralogy of asteroids. In *Asteroids III* (W. F. Bottke Jr. et al., eds.), this volume. Univ. of Arizona, Tucson.

Gehrels T. (1956) Photometric studies of asteroids. V. The light-curve and phase function of 20 Massalia. *Astrophys. J., 123,* 331–338.

Gehrels T. (1967) Minor planets. I. The rotation of Vesta. Photometric studies of asteroids. *Astron. J., 72,* 929–938.

Gehrels T. and Taylor R. C. (1977) Minor planets and related objects. XXII. Phase functions for (6) Hebe. *Astron. J., 82,* 229–237.

Gradie J., Veverka J., and Buratti B. (1980) The effects of scattering geometry on the spectrophotometric properties of powdered material. *Proc. Lunar Planet. Sci. Conf. 11th,* pp. 799–815.

Hapke B. (1986) Bidirectional reflectance spectroscopy: 4. The extinction coefficient and the opposition effect. *Icarus, 67,* 264–280.

Hapke B. (1990) Coherent backscatter and the radar characteristics of outer planet satellites. *Icarus, 88,* 407–417.

Hapke B. (1993) *Theory of Reflectance and Emittance Spectroscopy.* Cambridge Univ., New York. 450 pp.

Hapke B. (1996) Are planetary regolith particles back scattering? Response to a paper by M. Mishchenko. *J. Quant. Spectr. Rad. Transfer, 55,* 837–848.

Hapke B. W., Nelson R. M., and Smythe W. D. (1993) The opposition effect of the Moon: The contribution of coherent backscatter. *Science, 260,* 509–511.

Hapke B., Nelson R., and Smythe W. (1998) The opposition effect of the Moon: Coherent backscatter and shadow hiding. *Icarus, 133,* 89–97.

Harris A. W. and Young J. W. (1989) Asteroid lightcurve observations from 1979–1981. *Icarus, 81,* 314–364.

Harris A. W., Young J. W., Bowell E., Martin L. J., Millis R. L., Poutanen M., Scaltriti F., Zappalà V., Schober H.-J., Debehogne H., and Zeigler K. W. (1989a) Photoelectric observations of asteroids 3, 24, 60, 261, and 863. *Icarus, 77,* 171–186.

Harris A. W., Young J. W., Contreiras L., Dockweiler T., Belkora L., Salo H., Harris W. D., Bowell E., Poutanen M., Binzel R. P., Tholen D. J., and Wang S. (1989b) Phase relations of high albedo asteroids: The unusual opposition brightening of 44 Nysa and 64 Angelina. *Icarus, 81,* 365–374.

Helfenstein P., Veverka J., Thomas P. C., Simonelli D. P., Lee P., Klaasen K., Johnson T. V., Breneman H., Head J. W., Murchie S., Fanale F., Robinson M., Clark B., Granahan J., Garbeil H., McEwen A. S., Kirk R. L., Davies M., Neukum G., Mottola S., Wagner R., Belton M., Chapman C., and Pilcher C. (1994) Galileo photometry of asteroid 951 Gaspra. *Icarus, 107,* 37–60.

Helfenstein P., Veverka J., Thomas P. C., Simonelli D. P., Klaasen K., Johnson T. V., Fanale F., Granahan J., McEwen A. S., Belton M., and Chapman C. (1996) Galileo photometry of asteroid 243 Ida. *Icarus, 120,* 48–65.

Hillier J. K. (1997) Shadow-hiding opposition surge for a two-layer surface. *Icarus, 128,* 15–27.

Jedicke R., Larsen J., and Spahr T. (2002) Observational selection effects in asteroid surveys. In *Asteroids III* (W. F. Bottke Jr. et al., eds.), this volume. Univ. of Arizona, Tucson.

Kaasalainen M., Torppa J., and Muinonen K. (2001) Optimization methods for asteroid lightcurve inversion. II. The complete inverse problem. *Icarus, 153,* 37–51.

Kaasalainen M., Mottola S., and Fulchignoni M. (2002) Asteroid models from disk-integrated data. In *Asteroids III* (W. F. Bottke Jr. et al., eds.), this volume. Univ. of Arizona, Tucson.

Kaasalainen S., Piironen J., Muinonen K., Karttunen H., Peltoniemi J. I., and Näränen J. (2002) Experiments of backscattering from regolith-type samples. In *Electromagnetic and Light Scattering by Non-Spherical Particles, Gainesville 2002* (B. Gustafson et al., eds.), pp. 143–146. Army Research Laboratory, Adelphi, Maryland.

Kamei A. and Nakamura A. M. (2002) Laboratory study of bidirectional reflectance of powdered surfaces: On the asymmetry parameter of asteroid photometric data. *Icarus,* in press.

Karttunen H. and Bowell E. (1989) Modelling asteroid brightness variations II. The uninterpretability of light curves and phase curves. *Astron. Astrophys., 208,* 320–326.

Kiselev N. N., Lupishko D. F., Chernova G. P., and Shkuratov Yu. G. (1990) Polarimetry of asteroid 1685 Toro. *Kin. Phys. Neb. Tel., 6,* 77–82 (in Russian).

Kiselev N. N., Chernova G. P., and Lupishko D. F. (1994) Polarimetry of asteroids 1036 Ganymed and 1627 Ivar. *Kin. Phys. Neb. Tel., 10,* 35–39 (in Russian).

Kiselev N. N., Shakhovskoy N. M., and Efimov Yu. S. (1996) On the polarization opposition effect of E-type asteroid 64 Angelina. *Icarus, 120,* 408–411.

Kiselev N. N., Rosenbush V. K., and Jockers K. (1999) Polarimetry of asteroid 2100 Ra-Shalom at large phase angle. *Icarus, 140,* 464–466.

Kolokolova L. O., Mishchenko M. I., and Wolff M. (1993) On the negative polarization of light scattered by subwavelength

regolith grains. *Mon. Not. R. Astron. Soc., 260,* 550–552.
Krugly Yu. N., Shevchenko V. G., Velichko F. P., Bowell E., Piironen J., Kwiatkowski T., Kryszczyńska A., and Michałowski T. (1994) Asteroid 83 Beatrix — photometry and model. *Astron. Astrophys. Suppl. Ser., 108,* 143–149.
Lagerkvist C.-I. and Magnusson P. (1990) Analysis of asteroid lightcurves. II. Phase curves in a generalized HG-system. *Astron. Astrophys. Suppl. Ser., 78,* 519–532.
Lagerkvist C.-I., Piironen J., and Erikson A., eds. (2001) *Asteroid Photometric Catalogue,* 5th edition. Astronomical Observatory, Uppsala University, Sweden. 201 pp.
Le Bertre T. and Zellner B. (1980) Surface texture of Vesta from optical polarimetry. *Icarus, 43,* 172–180.
Lumme K. and Bowell E. (1981) Radiative transfer in the surfaces of atmosphereless bodies. I. Theory. *Astron. J., 86,* 1694–1704.
Lumme K., Peltoniemi J. I., and Irvine W. M. (1990) Diffuse reflection in stochastically bounded semi-infinite media. *Trans. Theory Stat. Phys., 19,* 317–332.
Lumme K., Rahola J., and Hovenier J. W. (1997) Light scattering by dense clusters of spheres. *Icarus, 126,* 455–469.
Lupishko D. F. (1999) Photometry and polarimetry of asteroids: Results of observations and data analysis. Doctor's thesis, Kharkov National University. 259 pp.
Lupishko D. F. and Di Martino M. (1998) Physical properties of near-Earth asteroids. *Planet. Space Sci., 46,* 47–74.
Lupishko D. F. and Kiselev N. N. (1995) Inversion effect of spectral dependences of asteroid polarization (abstract). *Bull. Am. Astron. Soc., 27,* 1064.
Lupishko D. F. and Mohamed R. A. (1996) A new calibration of the polarimetric albedo scale of asteroids. *Icarus, 119,* 209–213.
Lupishko D. F. and Vasilyev S. V. (1997) Asteroid polarimetric database. *Kin. Phys. Neb. Tel., 13,* 17–23.
Lupishko D. F., Belskaya I. N., and Kvaratshelia O. I. (1988) Polarimetry of Vesta in 1986 opposition. *Astron. Vestnik, XXII:2,* 142–146.
Lupishko D. F., Efimov Yu. S., and Shakhovskoy N. M. (1991) Ceres' peculiar polarization (abstract). In *23rd Annual Meeting of the DPS of the AAS,* p. 184. Palo Alto, California.
Lupishko D. F., Kiselev N. N., Chernova G. P., Shakhovskoj N. M., and Vasilyev S. V. (1994) Polarization phase dependences of asteroids 55 Pandora and 704 Interamnia. *Kin. Phys. Neb. Tel., 10,* 40–44.
Lupishko D. F., Vasilyev S. V., Efimov Yu. S., and Shakhovskoj N. M. (1995) UBVRI-polarimetry of asteroid 4179 Toutatis. *Icarus, 113,* 200–205.
Lupishko D. F., Efimov Yu. S., and Shakhovskoj N. M. (1999) Position angle variations of the polarization plane of asteroid 4 Vesta. *Solar System Res., 33,* 45–48.
Lyot B. (1929) Recherches sur la polarisation de la lumière des planètes et de quelques substances terrestres. *Ann. Obs. Paris, 8(1),* 1–161.
Magnusson P., Dahlgren M., Barucci M. A., Jorda L., Binzel R. P., Slivan S. M., Blanco C., Riccioli D., Buratti B. J., Colas F., Berthier J., De Angelis G., Di Martino M., Dotto E., Drummond J. D., Fink U., Hicks M., Grundy W., Wisniewski, W., Gaftonyuk N. M., Geyer E. H., Bauer T., Hoffmann M., Ivanova V., Komitov B., Donchev Z., Denchev P., Krugly Yu. N., Velichko F. P., Chiorny V. G., Lupishko D. F., Shevchenko V. G., Kwiatkowski T., Kryszczyńska A., Lahulla J. F., Licandro J., Mendez O., Mottola S., Erikson A., Ostro S. J., Pravec P., Pych W., Tholen D. J., Whiteley R., Wild W. J., Wolf M., and Šarounová L. (1996) Photometric observations and modeling of asteroid 1620 Geographos. *Icarus, 123,* 227–244.
McGuire A. F. and Hapke B. W. (1995) An experimental study of light scattering by large, irregular particles. *Icarus, 113,* 134–155.
Migliorini F., Manara A., Scaltriti F., Farinella P., Cellino A., and Di Martino M. (1997) Surface properties of (6) Hebe: A possible parent body of ordinary chondrites. *Icarus, 128,* 104–113.
Mishchenko M. I. (1994) Asymmetry parameters of the phase function for densely packed scattering grains. *J. Quant. Spectr. Rad. Transfer, 52,* 95–110.
Mishchenko M. I. (1996a) Diffuse and coherent backscattering by discrete random media — I. Radar reflectivity, polarization ratios, and enhancement factors for a half-space of polydisperse, nonabsorbing and absorbing spherical particles. *J. Quant. Spectr. Rad. Transfer, 56,* 673–702.
Mishchenko M. I. (1996b) Coherent backscattering by two-sphere clusters. *Opt. Lett., 21,* 623–625.
Mishchenko M. I. and Dlugach J. M. (1993) Coherent backscatter and the opposition effect for E-type asteroids. *Planet. Space Sci., 41,* 173–181.
Mishchenko M. I., Luck J.-M., and Nieuwenhuizen T. M. (2000) Full angular profile of the coherent polarization opposition effect. *J. Opt. Soc. Am., A17,* 888–891.
Mottola S., Erikson A., Harris A. W., Hahn G., Neukum G., Buie M. W., Sears W. D., Harris A. W., Tholen D. J., Whiteley R. J., Magnusson P., Piironen J., Kwiatkowski T., Borczyk W., Howell E. S., Hicks M. D., Fevig R., Krugly Yu. N., Velichko F. P., Chiorny V. G., Gaftonyuk N. M., Di Martino M., Pravec P., Šarounová L., Wolf M., Worman W., Davies J. K., Schober H.-J., and Pych W. (1997) Physical model of near-earth asteroid 6489 Golevka (1991 JX) from optical and infrared observations. *Astron. J., 114,* 1234–1245.
Muinonen K. (1989) Electromagnetic scattering by two interacting dipoles. In *Proc. 1989 URSI Electromagnetic Theory Symposium,* pp. 428–430. Stockholm, Sweden.
Muinonen K. (1990) Light scattering by inhomogeneous media: Backward enhancement and reversal of polarization. Ph.D. thesis, University of Helsinki.
Muinonen K. (1994) Coherent backscattering by solar system dust particles. In *Asteroids, Comets and Meteors 1993* (A. Milani et al., eds.), pp. 271–296. Kluwer, Dordrecht.
Muinonen K. (2000) Light scattering by stochastically shaped particles. In *Light Scattering by Nonspherical Particles: Theory, Measurements, and Applications* (M. I. Mishchenko et al., eds.), pp. 323–352. Academic, San Diego.
Muinonen K. (2002) Coherent backscattering by absorbing and scattering media. In *Electromagnetic and Light Scattering by Non-Spherical Particles, Gainesville 2002* (B. Gustafson et al., eds.), pp. 223–226. Army Research Laboratory, Adelphi, Maryland.
Muinonen K. and Lumme K. (1991) Light scattering by solar system dust: The opposition effect and the reversal of linear polarization. In *Origin and Evolution of Dust in the Solar System* (A.-C. Levasseur-Regourd and H. Hasekawa, eds.), pp. 159–162. IAU Colloquium 126, Kluwer, Dordrecht.
Muinonen K. O., Sihvola A. H., Lindell I. V., and Lumme K. A. (1991) Scattering by a small object close to an interface II. Study of backscattering. *J. Opt. Soc. Am., A8,* 477–482.
Muinonen K., Stankevich D., Shkuratov Yu. G., Kaasalainen S.,

and Piironen J. (2001) Shadowing effect in clusters of opaque spherical particles. *J. Quant. Spectr. Rad. Transfer, 70,* 787–810.

Muinonen K., Piironen J., Kaasalainen S., and Cellino A. (2002a) Asteroid photometric and polarimetric phase curves: Empirical modeling. *Mem. S. A. It.,* in press.

Muinonen K., Videen G., Zubko E., and Shkuratov Yu. (2002b) Numerical techniques for coherent backscattering by random media. In *Cosmic Dust and Its Optics: Bratislava Contributions* (G. Videen and M. Kocifaj, eds.), pp. 261–282. Kluwer, Dordrecht.

Muinonen K., Shkuratov Yu. G., Ovcharenko A., Piironen J., Stankevich D., Miloslavskaya O., Kaasalainen S., and Josset J.-L. (2002c) The SMART-1 AMIE experiment: Implication to the lunar opposition effect. *Planet. Space Sci.,* in press.

Mukai T., Iwata T., Kikuchi S., Hirata R., Matsumura M., Nakamura Y., Narusawa S., Okazaki A., Seki M., and Hayashi K. (1997) Polarimetric observations of 4179 Toutatis in 1992/1993. *Icarus, 127,* 452–460.

Nelson R., Hapke B., Smythe W., Shkuratov Yu., Ovcharenko A., and Stankevich D. (1999) The reflectance phase curves at very small phase angle: A comparative study of two goniometers (abstract). In *Lunar and Planetary Science XXX,* Abstract #2068. Lunar and Planetary Institute, Houston (CD-ROM).

Nelson R. M., Hapke B. W., Smythe W. D., and Spilker L. J. (2000) The opposition effect in simulated planetary regoliths. Reflectance and circular polarization ratio change at small phase angle. *Icarus, 147,* 545–558.

Nousiainen T., Muinonen K., and Räisänen P. (2002) Scattering of light by large Saharan dust particles in a modified ray-optics approximation. *J. Geophys. Res.,* in press.

Oetking P. (1966) Photometric studies of diffusely reflecting surfaces with applications to the brightness of the Moon. *J. Geophys. Res., 71,* 2505–2513.

Ovcharenko A. A. and Shkuratov Yu. G. (2000) Weak-localization effect for light backscattered by surfaces with a complex structure. *Opt. Spectrosc., 88,* 253–259.

Ozrin V. D. (1992) Exact solution for coherent backscattering of polarized light from a random medium of Rayleigh scatterers. *Waves Random Med., 2,* 141–164.

Peltoniemi J. I. (1993a) Light scattering in planetary regoliths and cloudy atmospheres. Ph.D. thesis, University of Helsinki, Finland.

Peltoniemi J. I. (1993b) Radiative transfer in stochastically inhomogeneous media. *J. Quant. Spectr. Rad. Transfer, 50,* 655–671.

Peltoniemi J. I. and Lumme K. (1992) Light scattering by closely packed particulate media. *J. Opt. Soc. Am., A9,* 1320–1326.

Piironen J., Bowell E., Erikson A., and Magnusson P. (1994) Photometry of eleven asteroids at small phase angles. *Astron. Astrophys. Suppl. Ser., 106,* 587–595.

Piironen J., Muinonen K., Nousiainen T., Sasse C., Roth S., and Peltoniemi J. I. (1998) Albedo measurements on meteorite particles. *Planet. Space Sci., 46,* 937–943.

Piironen J., Muinonen K., Keränen S., Karttunen H., and Peltoniemi J. I. (2000) Backscattering of light by snow: Field measurements. In *Observing Land From Space: Science, Customers and Technology, Advances in Global Change Research 4* (M. M. Verstraete et al., eds.), pp. 219–229. Kluwer, Dordrecht.

Poutanen M. (1983) UBV photometry of asteroid 64 Angelina. In *Asteroids, Comets, Meteors* (C.-I. Lagerkvist and H. Rickman, eds.), pp. 45–48. Uppsala Universitet, Uppsala.

Poutanen M., Bowell E., Martin L. J., and Thompson D. T. (1985) Photoelectric photometry of (69) Hesperia. *Astron. Astrophys. Suppl. Ser., 61,* 291–297.

Pravec P., Wolf M., Šarounová L., Mottola S., Erikson A., Hahn G., Harris A. W., and Young J. W. (1997) The near-Earth objects follow-up program. II. Results for 8 asteroids from 1982 to 1995. *Icarus, 130,* 275–286.

Rosenbush V. K., Avramchuk V. V., Rosenbush A. E., and Mishchenko M. I. (1997) Polarization properties of the Galilean satellites of Jupiter: Observations and preliminary analysis. *Astrophys. J., 487,* 402–414.

Rosenbush V. K., Kiselev N. N., Avramchuk V. V., Jockers K., Shakhovskoj N. M., and Efimov Yu. S. (2002) Coherent effects in light scattering from atmosphereless solar system bodies. In *Electromagnetic and Light Scattering by Non-Spherical Particles, Gainesville 2002* (B. Gustafson et al., eds.), pp. 279–282. Army Research Laboratory, Adelphi, Maryland.

Sasse C., Muinonen K., Piironen J., and Dröse G. (1996) Albedo measurements on single particles. *J. Quant. Spectr. Rad. Transfer, 55,* 673–681.

Scaltriti F., Zappalà V., and Stanzel R. (1978) Lightcurves, phase function and pole of the asteroid 22 Kalliope. *Icarus, 34,* 93–98.

Shepard M. K. and Arvidson R. E. (1999) The opposition surge and photopolarimetry of fresh and coated basalts. *Icarus, 141,* 172–178.

Shepard M. K. and Campbell B. A. (1998) Shadows on a planetary surface and implications for photometric roughness. *Icarus, 134,* 279–291.

Shevchenko V. G., Chiorny V. G., Kalashnikov A. V., Krugly Yu. N., Mohamed R. A., and Velichko F. P. (1996) Magnitude-phase dependences for three asteroids. *Astron. Astrophys. Suppl. Ser., 115,* 475–479.

Shevchenko V. G., Belskaya I. N., Chiorny V. G., Piironen J., Erikson A., Neukum G., and Mohamed R. (1997) Asteroid observations at low phase angles. I. 50 Virginia, 91 Aegina, and 102 Miriam. *Planet. Space Sci., 45,* 1615–1623.

Shevchenko V. G., Belskaya I. N., Krugly Yu. N., Chiorny V. G., and Gaftonyuk N. M. (2002) Asteroid observations at low phase angles. II. 5 Astraea, 75 Eurynome, 77 Frigga, 105 Artemis, 119 Althaea, 124 Alkeste, and 201 Penelope. *Icarus,* in press.

Shkuratov Yu. G. (1985) On the origin of the opposition effect and negative polarization for cosmic bodies with solid surface. *Astron. Circular No. 1400,* pp. 3–6. Sternberg State Astronomical Institute, Moscow.

Shkuratov Yu. G. (1987) Negative polarization of sunlight scattered from celestial bodies: Interpretation of the wavelength dependence. *Sov. Astron. Lett., 13,* 182–183.

Shkuratov Yu. G. (1989) A new mechanism of the negative polarization of light scattered by the surfaces of atmosphereless celestial bodies. *Astron. Vestnik, 23,* 176–180.

Shkuratov Yu. (1991) An interference model of the negative polarization of light scattered by atmosphereless celestial bodies. *Solar System Res., 25,* 134–142.

Shkuratov Yu. G. and Helfenstein P. (2001) The opposition effect and the quasi-fractal structure of regolith: Theory. *Icarus, 152,* 96–116.

Shkuratov Yu. G. and Muinonen K. (1992) Interpreting asteroid photometry and polarimetry using a model of shadowing and

coherent backscattering. In *Asteroids, Comets, Meteors 1991* (A. W. Harris and E. Bowell, eds.), pp. 549–552. Flagstaff, Arizona.

Shkuratov Yu. G. and Opanasenko N. V. (1992) Polarimetric and photometric properties of the Moon: Telescope observation and laboratory simulation. 2. The positive polarization. *Icarus, 99,* 468–484.

Shkuratov Yu. G., Opanasenko N. V., and Kreslavsky M. A. (1992) Polarimetric and photometric properties of the Moon: Telescopic observations and laboratory simulations. 1. The negative polarization. *Icarus, 95,* 283–299.

Shkuratov Yu. G., Muinonen K., Bowell E., Lumme K., Peltoniemi J. I., Kreslavsky M. A., Stankevich D. G., Tishkovets V. P., Opanasenko N. V., and Melkumova L. Y. (1994) A critical review of theoretical models for the negative polarization of light scattered by atmosphereless solar system bodies. *Earth, Moon, Planets, 65,* 201–246.

Shkuratov Yu. G., Kreslavsky M. A., Ovcharenko A. A., Stankevich D. G., Zubko E. S., Pieters C., and Arnold G. (1999) Opposition effect from Clementine data and mechanisms of backscatter. *Icarus, 141,* 132–155.

Shkuratov Yu., Ovcharenko A., Zubko E., Stankevich D., Miloslavskaya O., Muinonen K., Piironen J., Nelson R., Smythe W., Rosenbush V., and Helfenstein P. (2002) The opposition effect and negative polarization of structural analogs of planetary regoliths. *Icarus,* in press.

Stankevich D. G., Shkuratov Yu. G., and Muinonen K. (1999) Shadow-hiding effect in inhomogeneous and layered particulate media. *J. Quant. Spectr. Rad. Transfer, 63,* 445–458.

Stankevich D., Grynko Ye., Shkuratov Yu., and Muinonen K. (2002) A computer simulation of multiple scattering of light rays in systems of opaque particles. *J. Quant. Spectr. Rad. Transfer,* in press.

Tedesco E., Drummond J., Gandy M., Birch P., Nikoloff I., and Zellner B. (1978) 1580 Betulia: An unusual asteroid with an extraordinary lightcurve. *Icarus, 35,* 344–359.

Tishkovets V. P. (2002) Multiple scattering of light by a layer of discrete random medium: backscattering. *J. Quant. Spectr. Rad. Transfer, 72,* 123–137.

Tishkovets V. P., Litvinov P. V., and Lyubchenko M. V. (2002) Coherent opposition effects for semi-infinite discrete random medium in the double-scattering approximation. *J. Quant. Spectr. Rad. Transfer, 72,* 803–811.

Verbiscer A. J. and Veverka J. (1995) Interpretation of the IAU two-parameter magnitude system for asteroids in terms of Hapke photometric theory. *Icarus, 115,* 369–373.

Veverka J., Thomas, P. C., Bell J. F. III, Bell M., Carcich B., Clark B., Harch A., Joseph J., Martin P., Robinson M., Murchie S., Izenberg N., Hawkins E., Warren J., Farquhar R., Cheng A., Dunham D., Chapman C., Merline W. J., MacFadden L., Wellnitz D., Malin M., Owen W. M. Jr., Miller J. K., Williams B. G., and Yeomans D. K. (1999) Imaging of asteroid 433 Eros during NEAR's flyby recoinnaisance. *Science, 285,* 562–564.

Veverka J., Robinson M., Thomas P., Murchie S., Bell J. F. III, Izenberg N., Chapman C., Harch A., Bell M., Carcich B., Cheng A., Clark B., Domingue D., Dunham D., Farquhar R., Caffey M. J., Hawkins E., Joseph J., Kirk R., Li H., Lucey P., Malin M., Martin P., MacFadden L., Merline W. J., Miller J. K., Owen W. M. Jr., Peterson C., Prockter L., Warren J., Wellnitz D., Williams B. G., and Yeomans D. K. (2000) NEAR at Eros: Imaging and spectral results. *Science, 289,* 2088–2097.

Videen G. (2002) Polarization opposition effect and second-order ray-tracing. *Appl. Opt.,* in press.

Volten H., Muñoz O., de Haan J. F., Vassen W., Hovenier J., Muinonen K., and Nousiainen T. (2001) Scattering matrices of mineral aerosol particles at 441.6 nm and 632.8 nm. *J. Geophys. Res., 106,* 17375–17401.

Wisniewski W. Z., Michałowski T. M., Harris A. W., and McMillan R. S. (1997) Photometric observations of 125 asteroids. *Icarus, 126,* 395–449.

Zappalà V., Cellino A., Barucci A. M., Fulchignoni M., and Lupishko D. F. (1990) An analysis of the amplitude-phase relationship among asteroids. *Astron. Astrophys., 231,* 548–560.

Zellner B. and Gradie J. (1976) Minor planets and related objects. XX. Polarimetric evidence for the albedos and compositions of 94 asteroids. *Astron. J., 81,* 262–280.

Zellner B., Gehrels T., and Gradie J. (1974) Minor planets and related objects. XVI. Polarimetric diameters. *Astron. J., 79,* 1100–1110.

Zellner B. H., Albrecht R., Binzel R. P., Gaffey M. J., Thomas P. C., Storrs A. D., and Wells E. N. (1997) Hubble Space Telescope images of asteroid 4 Vesta in 1994. *Icarus, 128,* 83–87.

Zubko Eu., Ovcharenko A., and Shkuratov Yu. G. (2002) Polarimetric weak-localization effect in scattering of natural light in the region of small phase angles. *Opt. Spectrosc., 92,* 443–448.